SUPPLEMENTARY INFORMATION

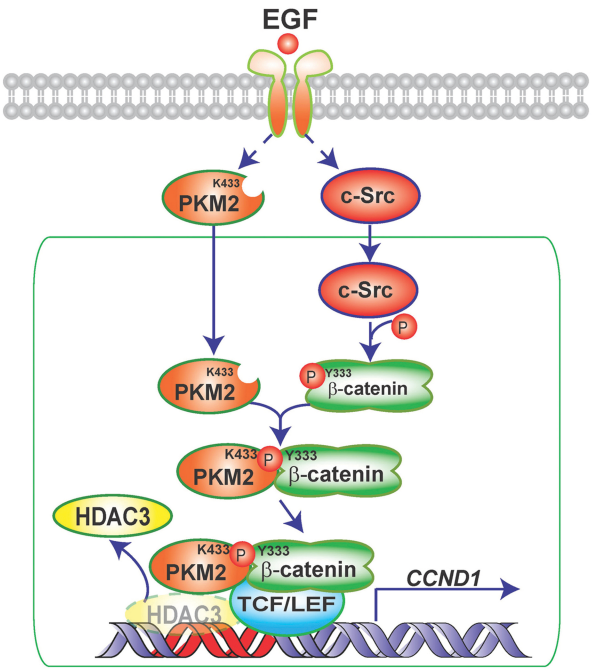

Supplementary Figure 1. **A mechanism for EGFR-induced β-catenin transactivation.** EGFR activation results in the translocation of PKM2 and c-Src to the nucleus. c-Src phosphorylates β-catenin at Y333 in the nucleus, leading to the interaction between PKM2 K433 and the phosphorylated Y333 residue of β-catenin. The binding of PKM2 to the *CCND1* promoter, which is likely guided by the associated β-catenin, is important for HDAC3 disassociation from the promoter and subsequent acetylation of histone H3. This protein complex, together with TCF/LEF, modulates cyclin D1 expression and promotes cell proliferation and tumorigenesis.

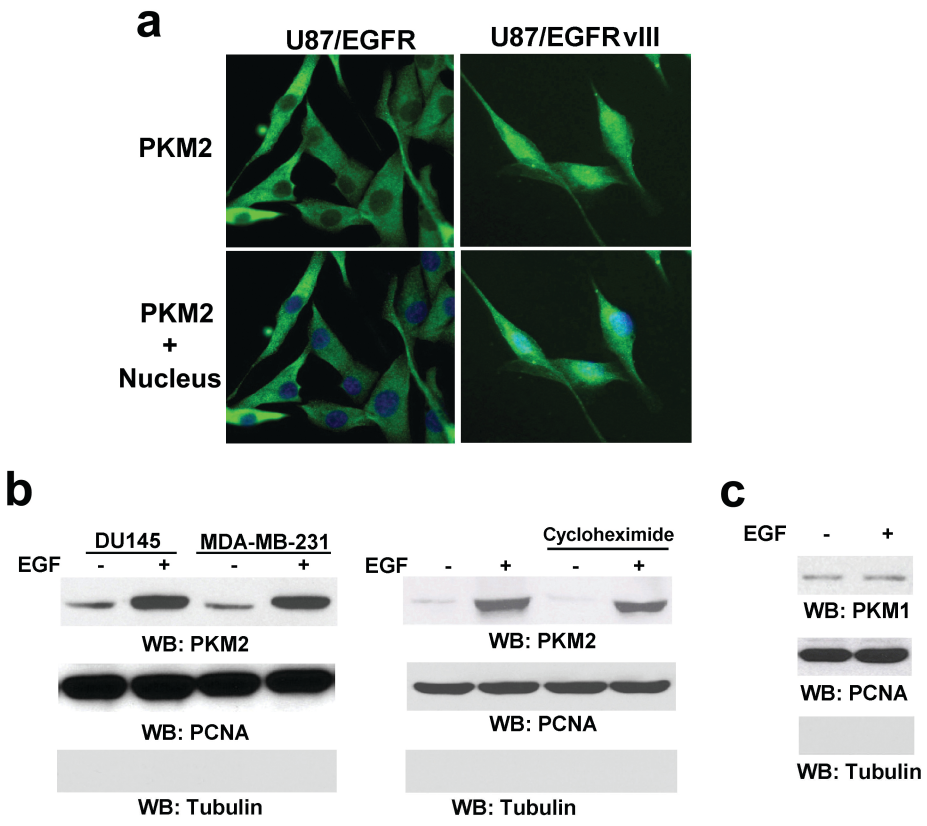

Supplementary Figure 2. EGFR activation induces nuclear translocation of PKM2.

Immunoblotting analyses (b, c) were performed with the indicated antibodies. Nuclear PCNA and cytoplasmic tubulin were used as controls.

a, The indicated cells were immunostained with an anti-PKM2 antibody. Nuclei were stained with Hoechst 33342 (blue)

b, The nuclear fractions were prepared from DU145, MDA-MB-231 (left panel), and U87/EGFR cells (right panel), which were pretreated with or without cycloheximide (CHX) (100 μg/ml) for 30 min before being treated with or without EGF (100 ng/ml) for 10 h.

c, The nuclear fractions were prepared from U87/EGFR cells, which had been treated with or without EGF (100 ng/ml) for 10 h.

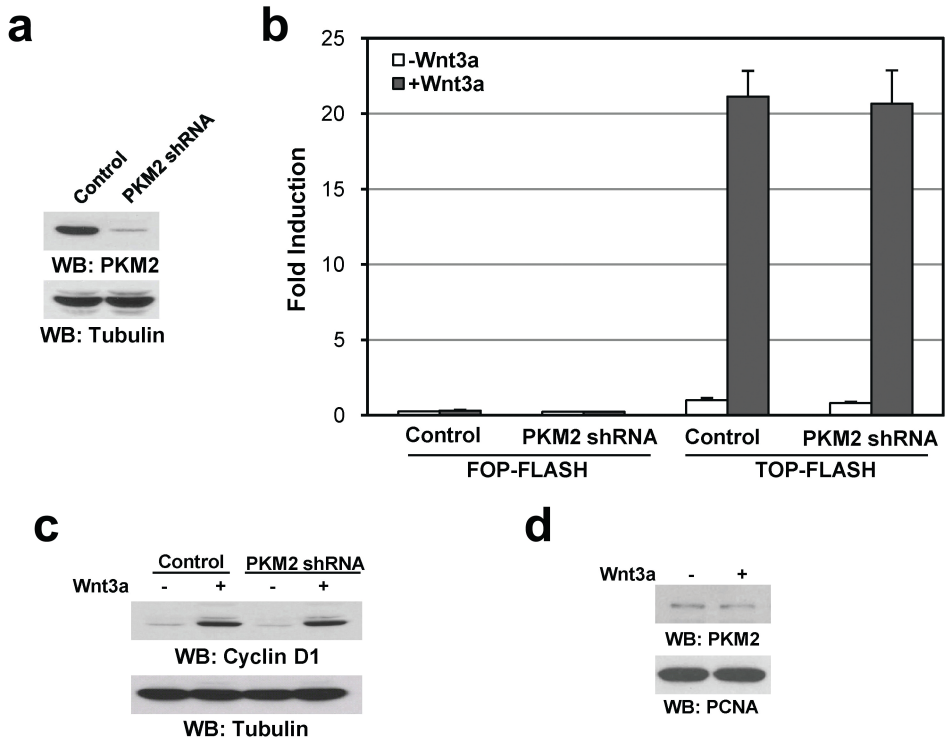

Supplementary Figure 3. PKM2 is not required for Wnt-induced β-catenin transactivation.

a, U87/EGFR cells were stably transfected with pGIPZ expressing a control or a *PKM2* shRNA.

b, U87/EGFR cells with or without PKM2 depletion were transfected with either TOP-FLASH or FOP-FLASH, which was followed by Wnt3a (20 ng/ml) treatment for 10 h. The relative levels of luciferase activity were normalized to the levels of untreated cells and to the levels of luciferase activity of the Renilla control plasmid. Data represent the means ± SD of three independent experiments.

c, U87/EGFR cells with or without PKM2 depletion were treated with or without Wnt3a (20 ng/ml) for 24 h.

d, U87/EGFR cells were treated with or without Wnt3a (20 ng/ml) for 10 h. The nuclear fractions were prepared.

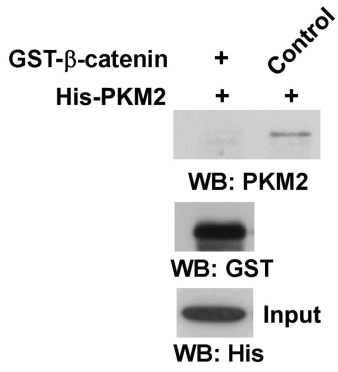

Supplementary Figure 4. PKM2 does not bind to β-catenin without post-translational modifications.

A GST pull-down assay was performed by mixing purified GST-β-catenin on glutathione agarose beads with purified His-PKM2 (left lane). Purified His-PKM2 was used as a positive control for the immunoblotting analysis (right lane).

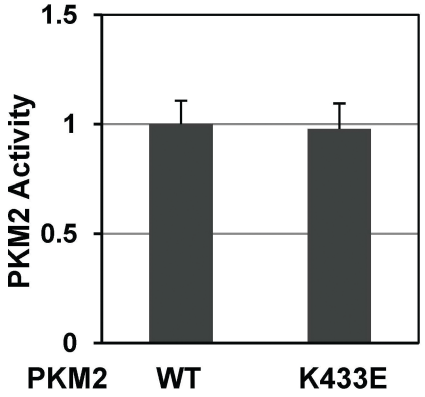

Supplementary Figure 5. PKM2 K433E has comparable enzyme activity to WT PKM2.

The activity of bacterially purified WT PKM2 (0.1 μg) and PKM2 K433E (0.1 μg) toward PEP in the presence of a saturated amount of the PKM2 activator fructose-1,6-bisphosphate (FBP) was measured using a pyruvate kinase assay. Data represent the means ± SD of three independent experiments

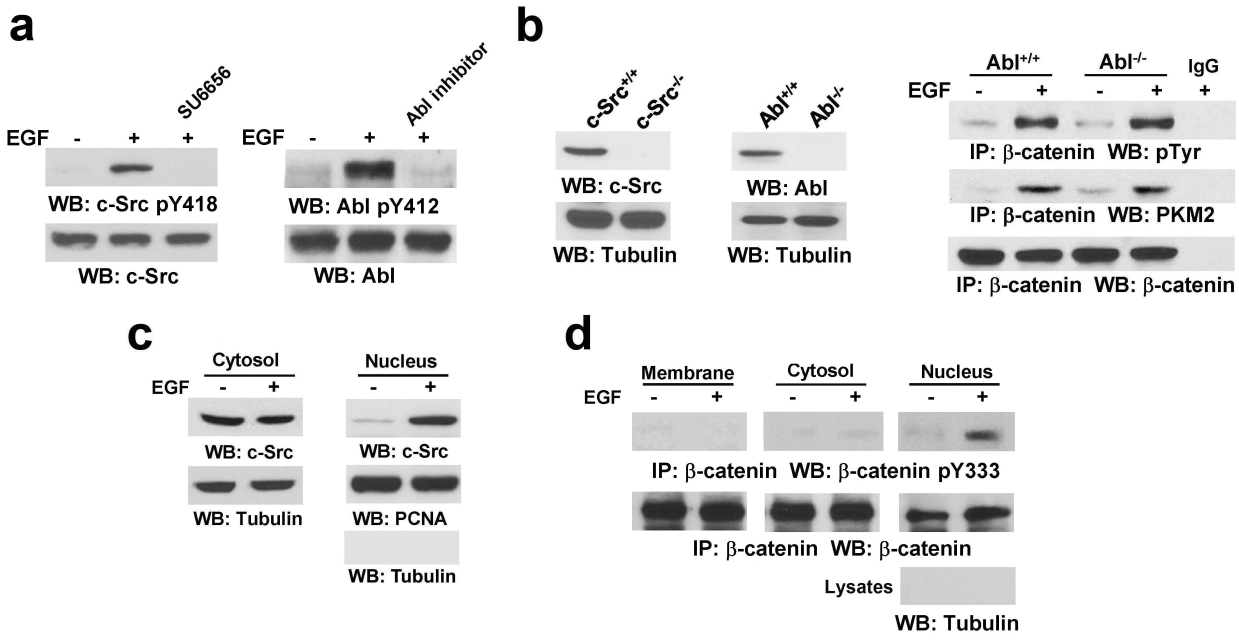

Supplementary Figure 6. EGF induces activation and nuclear translocation of c-Src and nuclear β-catenin phosphorylation.

Immunoprecipitation and immunoblotting analyses were performed with the indicated antibodies.

a, U87/EGFR cells were treated with SU6656 (4 μM) or an Abl inhibitor (0.2 μM) for 30 min before EGF (100 ng/ml) treatment for 6 h.

b, The indicated cells were treated with or without EGF (100 ng/ml) for 6 h.

c, Cytosolic or nuclear fractions of U87/EGFR cells treated with or without EGF (100 ng/ml) for 6 h were prepared.

d, β-catenin was immunoprecipitated from the membrane, cytosol, or nuclear fractions of U87/EGFR cells treated with or without EGF (100 ng/ml) for 6 h.

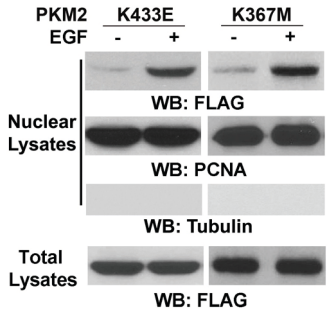

Supplementary Figure 7. PKM2 K433E and the inactive PKM2 K367M mutants translocated into the nucleus upon EGF stimulation.

U87/EGFR cells expressing FLAG-PKM2 K433E or FLAG-PKM2 K367M were treated with or without EGF (100 ng/ml) for 10 h. The nuclear fractions and total cell lysates were prepared. Immunoblotting analyses were performed with the indicated antibodies.

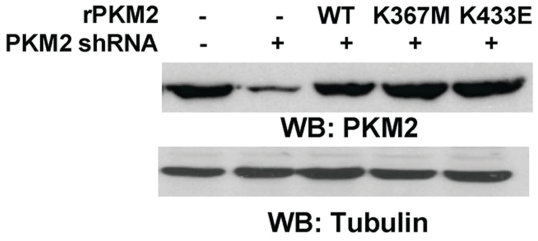

Supplementary Figure 8. Reconstituted expression of WT rPKM2, rPKM2 K367M, or rPKM2 in U87/EGFR cells with depleted endogenous PKM2

Cell lysates were prepared from the indicated cells. Immunoblotting analyses were performed with the indicated antibodies.

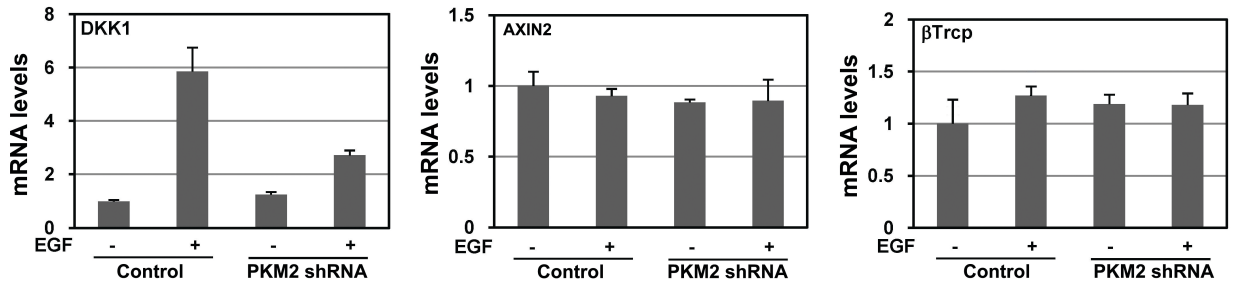

Supplementary Figure 9. EGF induces the β-catenin downstream effector gene DKK1, but not AXIN2 and βTrCP, in a PKM2-dependent manner.

U87/EGFR cells with or without PKM2 depletion were treated with or without EGF (100 ng/ml) for 24 h. mRNA expression levels of DKK1, AXIN2, and βTrCP were measured by real-time quantitative RT-PCR analysis. β-actin mRNA from the same cDNA library was amplified as a control. The relative mRNA levels of DKK1, AXIN2, and βTrCP were normalized to the levels of untreated cells and β-actin mRNA. Data represent the means ± SD of three independent experiments.

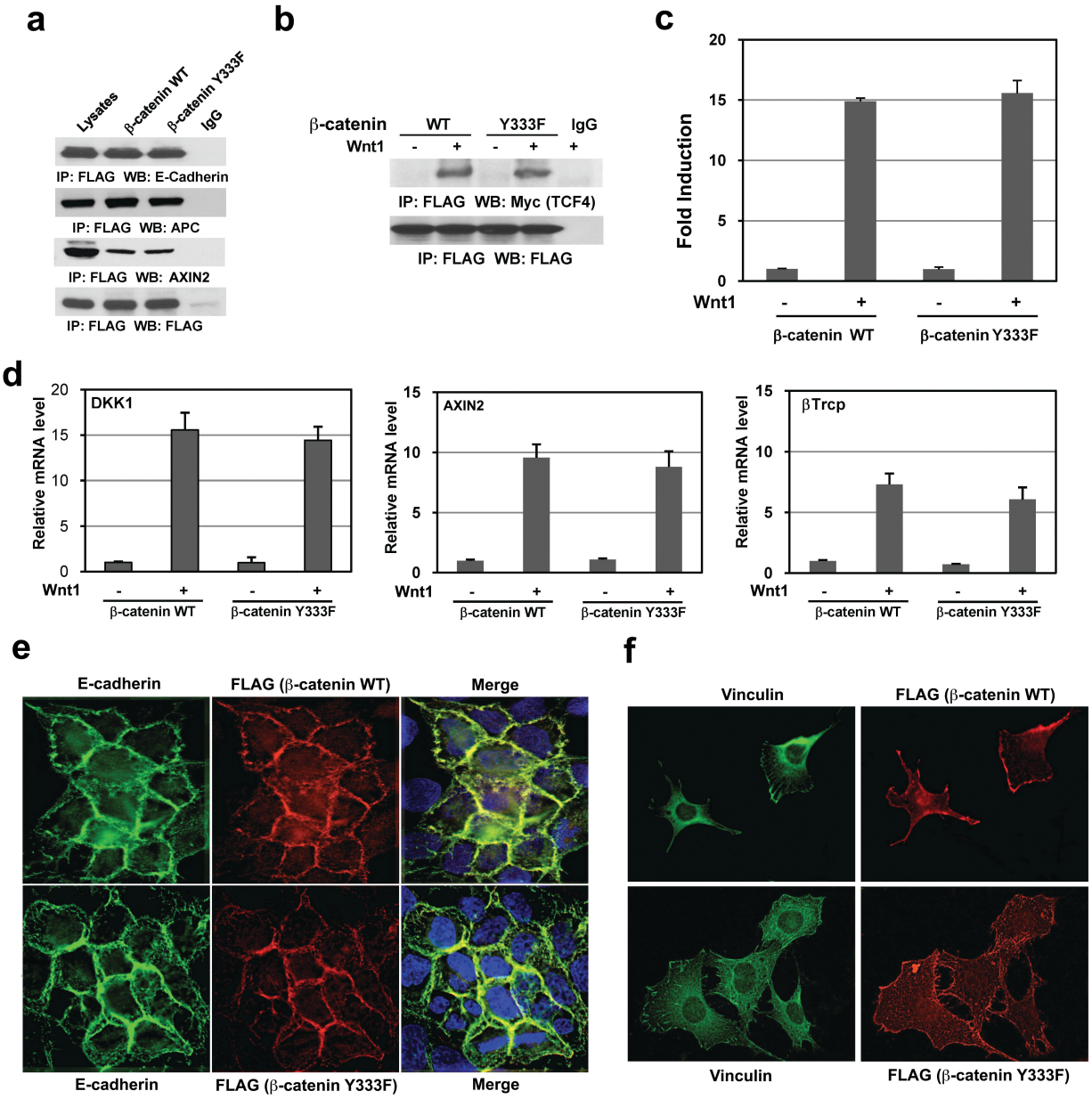
a
Lysates
β-catenin WT
β-catenin Y333F
IgG
IP: FLAG WB: E-Cadherin
IP: FLAG WB: APC
IP: FLAG WB: AXIN2
IP: FLAG WB: FLAG
b
β-catenin
WT
Y333F
IgG
Wnt1
IP: FLAG WB: Myc (TCF4)
IP: FLAG WB: FLAG
c
Fold Induction
Wnt1
β-catenin WT
β-catenin Y333F
d
DKK1
AXIN2
βTrcp
Relative mRNA level
e
E-cadherin
FLAG (β-catenin WT)
Merge
FLAG (β-catenin Y333F)
f
Vinculin
FLAG (β-catenin WT)
FLAG (β-catenin Y333F)

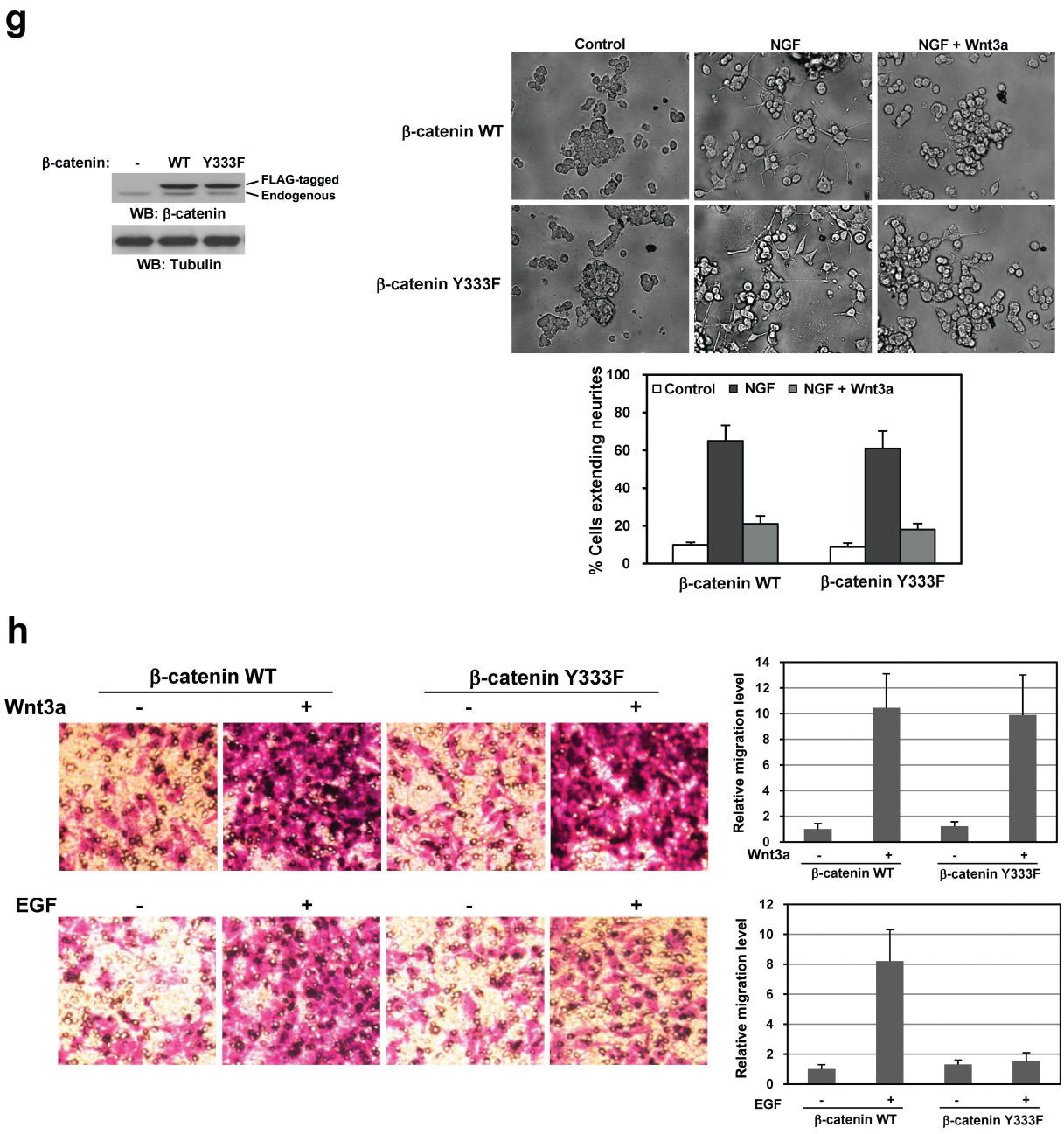

Supplementary Figure 10. β-catenin Y333 phosphorylation plays distinct roles in EGF and Wnt-induced signaling and biological activities.

a, β-catenin Y333F, like its WT counterpart, binds to APC, AXIN2, and E-cadherin. A vector expressing FLAG-β-catenin or FLAG-β-catenin Y333F was transiently transfected into A431 cells. Immunoprecipitation and immunoblotting analyses were performed with the indicated antibodies.

b, β-catenin Y333F, like its WT counterpart, increases its association with TCF4 upon Wnt1 expression. A vector expressing Myc-TCF4 was co-transfected with a vector expressing WT FLAG-β-catenin or FLAG-β-catenin Y333F into U87/EGFR cells. These cells were infected

with or without lentiviruses expressing Wnt1 for 72 h. Immunoprecipitation and immunoblotting analyses were performed with the indicated antibodies.

c, β-catenin Y333F behaves similarly to WT β-catenin in Wnt1-induced β-catenin transactivation. U87/EGFR cells with β-catenin depletion were reconstituted to express WT β-catenin or β-catenin Y333F. These cells were transfected with either TOP-FLASH or FOP-FLASH and infected with or without lentivirus expressing Wnt1 for 72 h. The relative levels of luciferase activity were normalized to the levels of untreated cells and to the levels of luciferase activity of the Renilla control plasmid. Data represent the means ± SD of three independent experiments.

d, β-catenin Y333F behaves similarly to WT β-catenin in Wnt1-induced expression of downstream target genes, such as AXIN2, DKK1, and βTrCP. U87/EGFR cells depleted of endogenous β-catenin were reconstituted to express WT rβ-catenin or rβ-catenin Y333F. These cells were infected with or without lentivirus expressing Wnt1 for 72 h. mRNA expression levels of DKK1, AXIN2, and βTrCP were measured by real-time quantitative RT-PCR analysis. β-actin mRNA from the same cDNA library was amplified as a control. The relative mRNA levels of DKK1, AXIN2, and βTrCP were normalized to the levels of untreated cells and β-actin mRNA. Data represent the means ± SD of three independent experiments.

e, β-catenin Y333F co-localizs with E-cadherin as does its WT counterpart. Immunofluorescence analyses of A431 cells expressing WT FLAG-β-catenin or FLAG-β-catenin Y333F were performed with the indicated antibodies. Nuclei were stained with Hoechst 33342 (blue).

f, β-catenin Y333F does not significantly alter focal adhesions, as detected by vinculin staining. Immunofluorescence analyses of NIH 3T3 cells expressing WT FLAG-β-catenin or FLAG-β-catenin Y333F were performed with the indicated antibodies.

g, There is no differences in the effects of WT β-catenin or β-catenin Y333F expression on Wnt3a-induced inhibition of nerve growth factor-stimulated neurite outgrowth of PC12 cells[27]. PC12 cells overexpressing WT FLAG-β-catenin or FLAG-β-catenin Y333 (immunoblotting analyses: left panel) were treated with or without Wnt3a (20 ng/ml) and/or nerve growth factor (NGF) (100 ng/ml) for 6 days. Pictures were taken with a digital camera mounted on a microscope with 100 × magnification (top right panel). Cells with neurite extensions longer than two cell diameter lengths were counted (bottom right panel). A total of 200 cells for each condition were examined.

h, β-catenin Y333F blocks EGF- but not Wnt3a-induced cell migration. U87/EGFR cells

depleted of endogenous β-catenin were reconstituted to express WT rβ-catenin or rβ-catenin Y333F. These cells were plated at the top surface of the Matrigel in the absence or presence of Wnt3a (20 ng/ml) or EGF (100 ng/ml). Twelve hours after plating, cells that had migrated to the opposite side of the insert were stained with crystal violet. Representative microphotographs are shown (left panel). The membranes with invaded cells were dissolved in 4% deoxycholic acid and read colorimetrically at 590 nm for quantification of invasion. Data represent the mean ± standard deviation of three independent experiments (right panel).

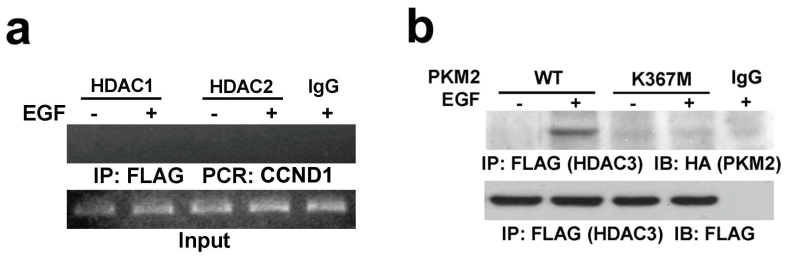

Supplementary Figure 11. HDAC1 or HDAC2 is not prebound to the *CCND1* Promoter, and HDAC3 interacts with PKM2.

a, U87/EGFR cells were treated with or without EGF (100 ng/ml) for 10 h. A ChIP assay was performed with antibodies for HDAC1 or HDAC2 for immunoprecipitation, followed by PCR with *CCND1* promoter-specific primers.

b, U87/EGFR cells transiently expressing FLAG-HDAC3 with WT HA-PKM2 or HA-PKM2 K367M were treated with or without EGF (100 ng/ml) for 10 h.

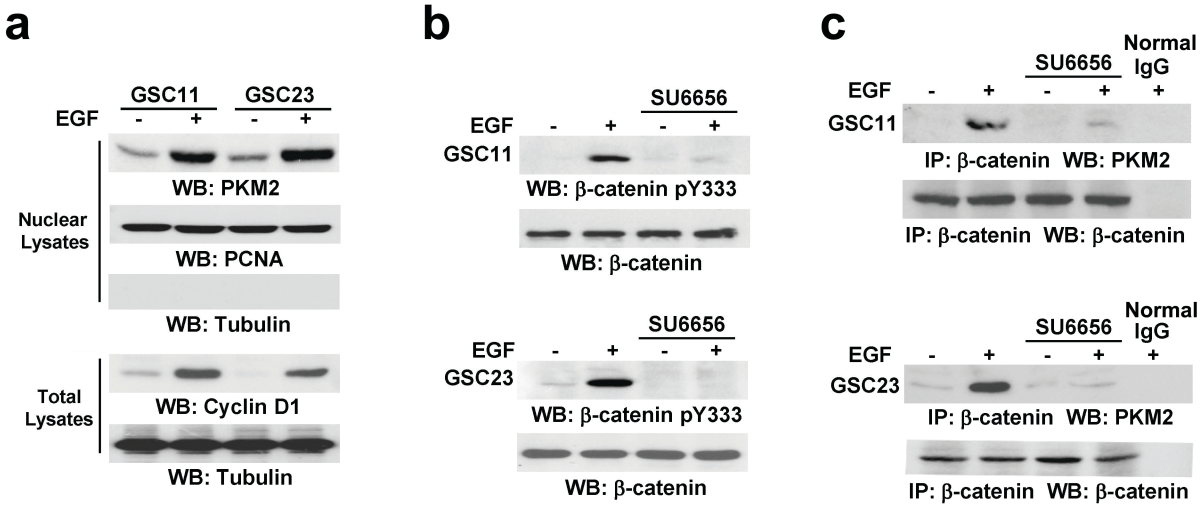

Supplementary Figure 12. EGF induces the nuclear translocation of PKM2, c-Src-dependent β-catenin Y333 phosphorylation, and a c-Src-dependent interaction between PKM2 and β-catenin in primary GBM cells.

Immunoprecipitation and immunoblotting analyses were performed with the indicated antibodies. Nuclear PCNA and cytoplasmic tubulin were used as controls.

a, The total cell lysates and nuclear fractions were prepared from the indicated primary GBM cells, which were treated with or without EGF (100 ng/ml) for 10 h (top panel) or 24 h (bottom panel).

b, c, The total cell lysates were prepared from the indicated primary GBM cells, which were pretreated with or without SU6656 (4 μM) for 30 min before being treated with or without EGF (100 ng/ml) for 6 h.

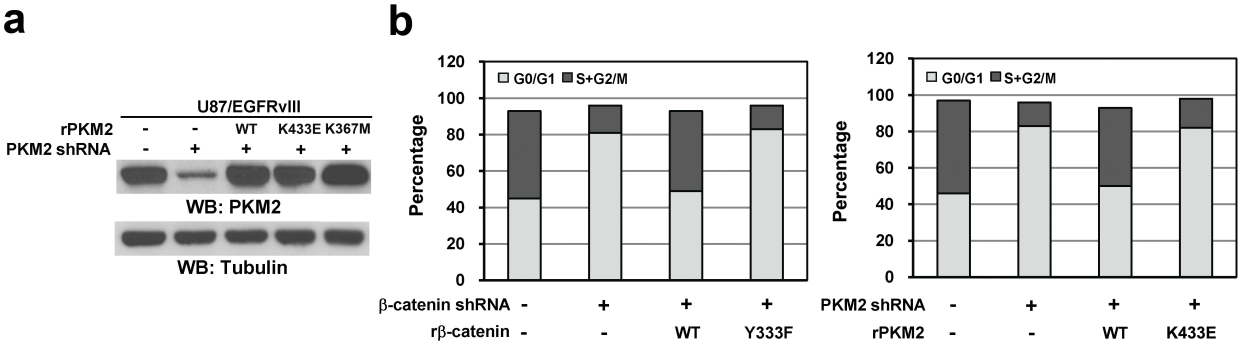

Supplementary Figure 13. The PKM2–β-catenin interaction is essential for cell cycle progression.

a, Expression of WT rPKM2, rPKM2 K433E, or rPKM2 K367M was reconstituted in U87/EGFRvIII cells with depleted PKM2. Immunoblotting analyses were performed with the indicated antibodies.

b, U87/EGFRvIII cells with or without depletion of β-catenin (left panel) and PKM2 (right panel) and reconstituted expression of WT rβ-catenin, rβ-catenin Y333F, WT rPKM2, or rPKM2 K433E were stained with propidium iodide and analyzed for DNA staining profiles by flow cytometry. Data represent the means ± SD of three independent experiments.

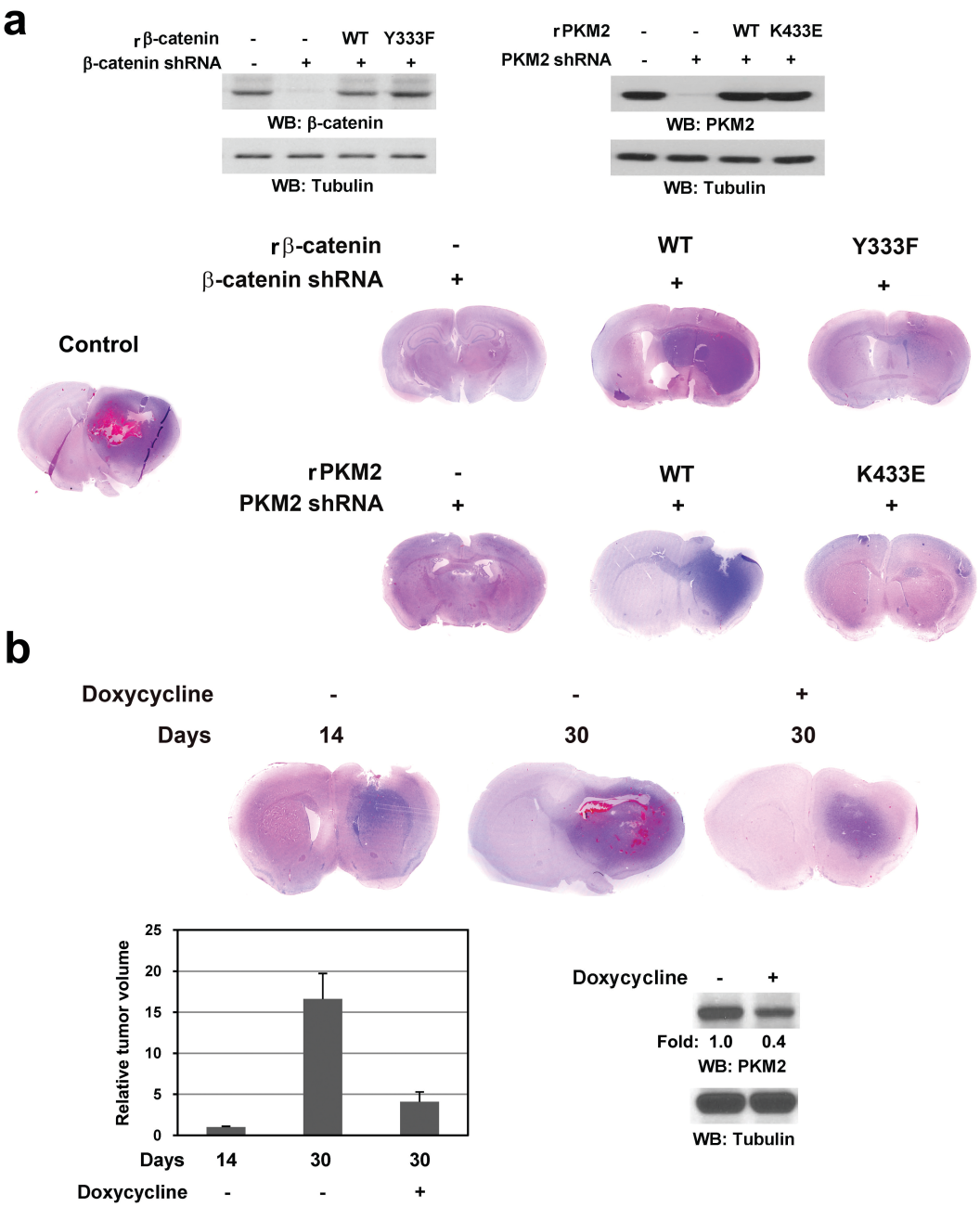

Supplementary Figure 14. PKM2-regulated β-catenin transactivation is required for brain tumor growth.

a, GSC11 cells (5×10^5) with or without RNAi-depleted β-catenin that were reconstituted to express WT rβ-catenin or rβ-catenin Y333, or GSC11 cells (5×10^5) with or without RNAi-depleted PKM2 that were reconstituted to express WT rPKM2 or rPKM2 K433E, were intracranially injected into athymic nude mice. After 30 days, the mice were sacrificed to examine tumor growth. H&E-stained coronal brain sections show representative tumor xenografts that were obtained for each group of mice. Immunoblotting analyses were performed with the indicated antibodies for the indicated cell lines (top panel).

b, GSC11 cells (5×10^5) that were infected with lentiviruses expressing PKM2 shRNA in a TRIPZ vector were intracranially injected into athymic nude mice for each group. After 14 days, 7 mice were sacrificed to examine tumor growth; the remaining mice that were fed with drinking water with or without doxycycline (800 μg/ml) were sacrificed at day 30. H&E-stained coronal brain sections showed representative tumor xenografts (top panel). Tumor volumes (bottom left panel) were estimated by measuring two dimensions [length (a) and width (b)] and calculated using the equation: $V = ab^2/2$. Immunoblotting analyses of protein lysates from the indicated tumor tissues were performed with the indicated antibodies (bottom right panel).

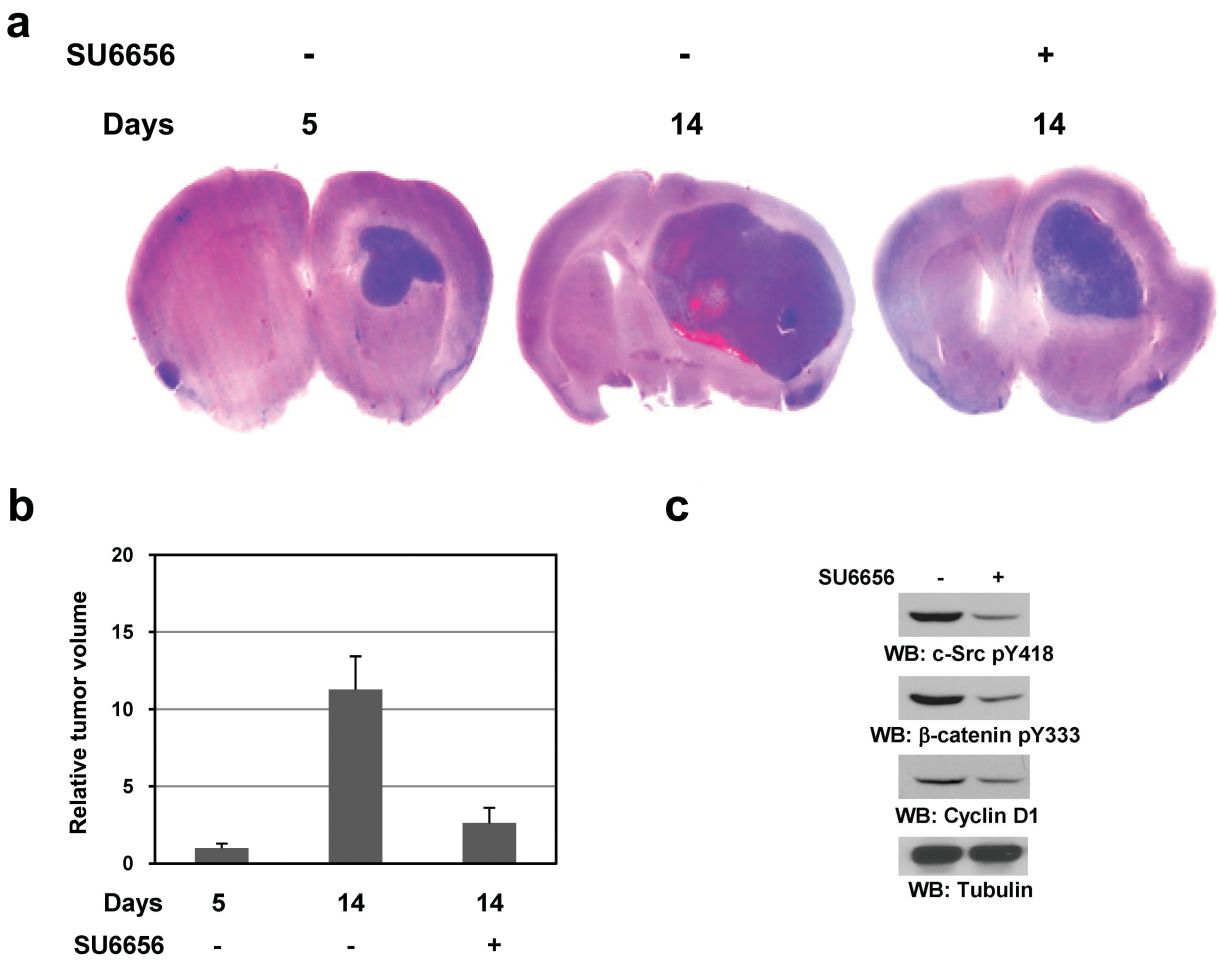

Supplementary Figure 15. c-Src inhibition suppresses tumorigenesis and reduces β-catenin Y333 phosphorylation and cyclin D1 expression in tumor tissues.

a, U87/EGFRvIII (5×10^5) cells were intracranially injected into athymic nude mice. After 5 days, 7 mice were sacrificed to examine tumor growth; the remaining mice, whose tumors were intracranially injected with SU6656 (0.015 mg/kg in 5 μl of DMSO) or DMSO every 3 days,

were sacrificed at day 15. H&E-stained coronal brain sections showed representative tumor xenografts.

b, Tumor volumes were measured using length (a) and width (b) and calculated using the equation: $V = ab^2/2$.

c, Immunoblotting analyses of the indicated tumor tissues were performed with the indicated antibodies.

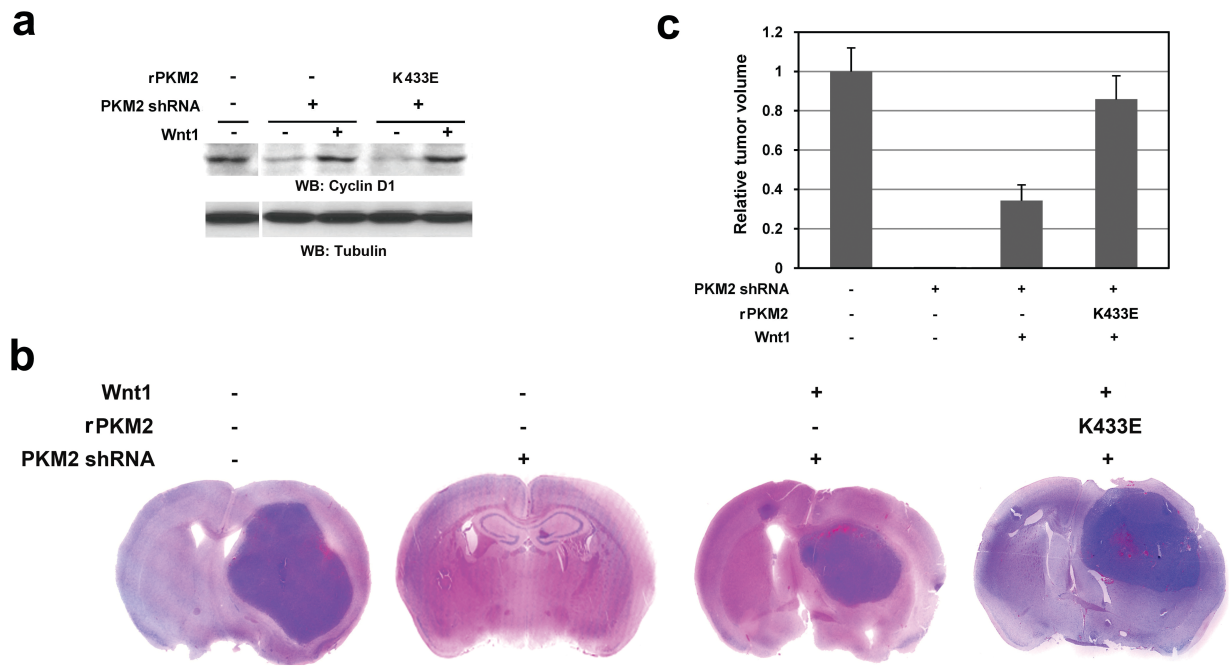

Supplementary Figure 16. Wnt1 expression rescues PKM2-dependent tumorigenesis.

a, U87/EGFRvIII-PKM2 shRNA cells with or without reconstituted expression of rPKM2 K433E were infected with lentiviruses expressing Wnt1 for 72 h. Immunoblotting analyses were performed with the indicated antibodies.

b, c, A total number of 5×10^5 U87/EGFRvIII cells with or without RNAi-depleted PKM2 and reconstitution of rPKM2 K433E expression were infected with or without lentiviruses expressing Wnt1 and intracranially injected into athymic nude mice. After two weeks, the mice were sacrificed to examine tumor growth. H&E-stained coronal brain sections showed representative tumor xenografts (b). (c) Tumor volumes were measured using two dimensions [length (a) and width (b)] and calculated using the equation: $V = ab^2/2$.

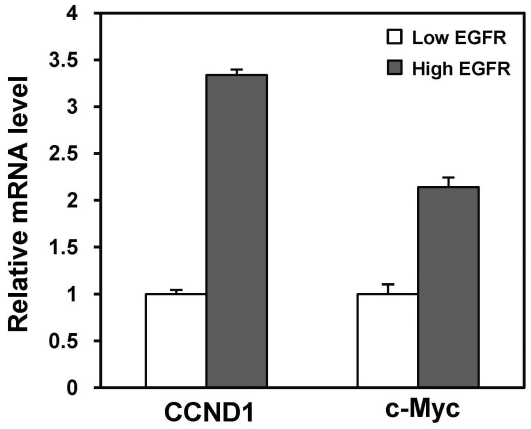

Supplementary Figure 17. EGFR Expression is correlated with *c-myc* and *CCND1* expression in human GBM samples

Publicly available microarray datasets (Affymetrix, U133) from TCGA and other sources were analyzed for relationships between *EGFR* expression and the expression of *c-myc* and *CCND1*. Normalized data for GBM samples were used to compare average gene expression levels of *c-myc* and *CCND1* in samples with an EGFR expression level of 5.0 or higher (n=204), versus expression of these genes in samples with *EGFR* expression levels of 2.0 or lower (n=403).

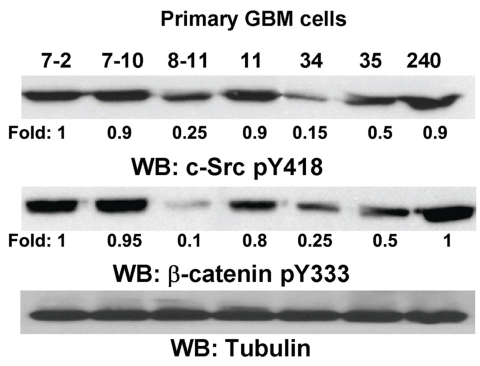

Supplementary Figure 18. The phosphorylation levels of β-catenin Y333 correlated with phosphorylation levels of activated c-Src in seven human primary GBM cell lines.

Immunoblotting analyses of lysates from seven lines of human primary GBM cells were performed with the indicated antibodies.

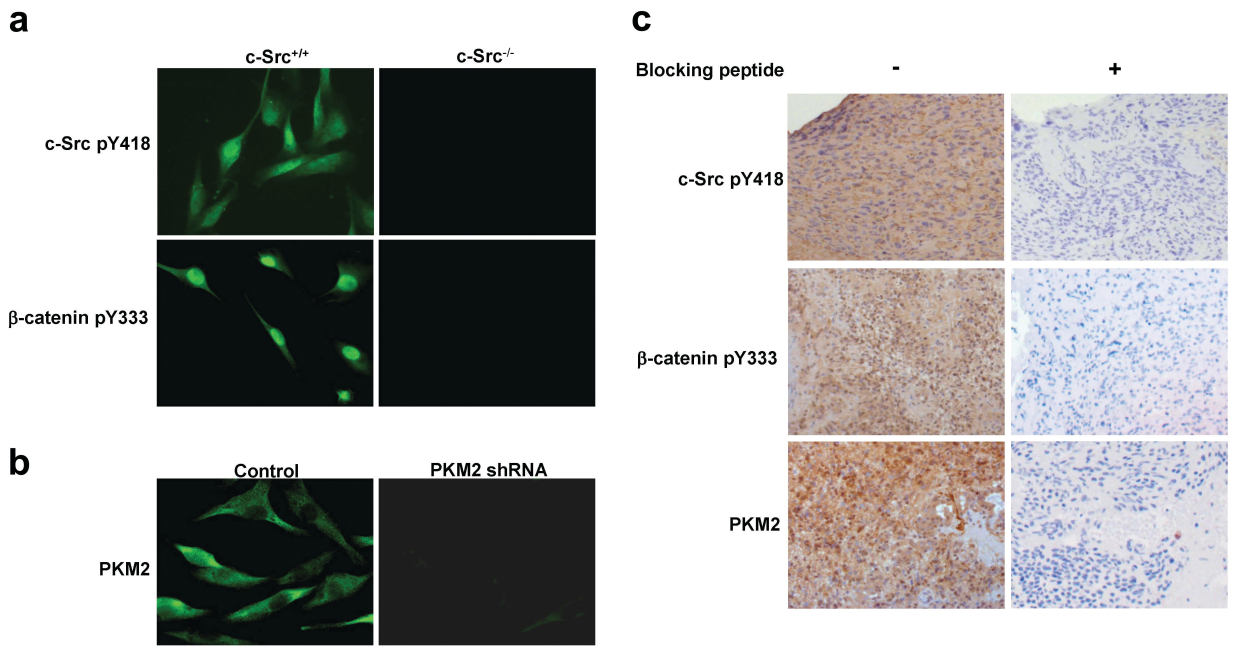

Supplementary Figure 19. Validation of antibody specificities.

Immunofluorescence and IHC analyses were performed with the indicated antibodies.

a, Immunofluorescence analyses of c-Src$^{+/+}$ and c-Src$^{-/-}$ cells were performed with the indicated antibodies. EGF induced phosphorylation of c-Src Y418 and β-catenin Y333 in c-Src$^{+/+}$, but not in c-Src$^{-/-}$, cells.

b, Immunofluorescence analyses of U87/EGFR with or without expression of shRNA PKM2 were performed with an anti-PKM2 antibody.

c, IHC analyses of human GBM tissues were performed with the indicated antibodies in the presence or absence of specific blocking peptides.

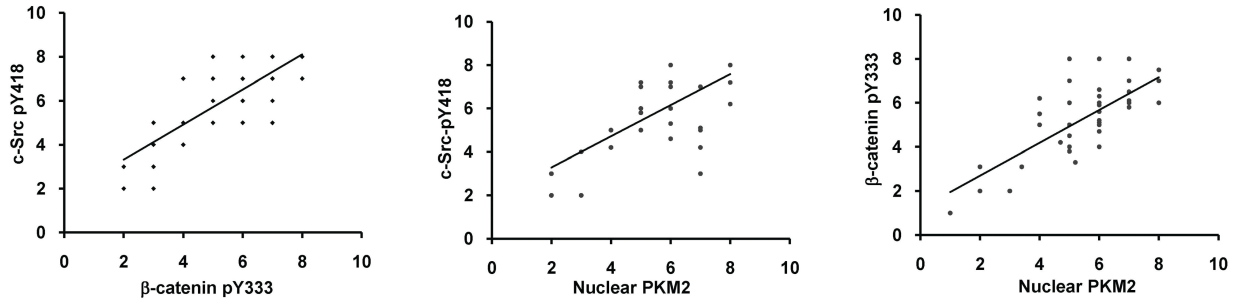

Supplementary Figure 20. The levels of c-Src Y418 phosphorylation, β-catenin Y333 phosphorylation, and nuclear expression of PKM2 are correlated with each other.

IHC staining with anti–phospho-c-Src Y418, anti–phospho-β-catenin Y333, and anti-PKM2 antibodies was performed on 55 GBM specimens. Semiquantitative scoring was performed (Pearson product moment correlation test; left panel, r = 0.81, $p < 0.00001$; middle panel, r = 0.70, $p < 0.0001$; right panel, r = 0.74, $p < 0.0001$). Note that some of the dots on the graphs represent more than one specimen (some scores overlapped).

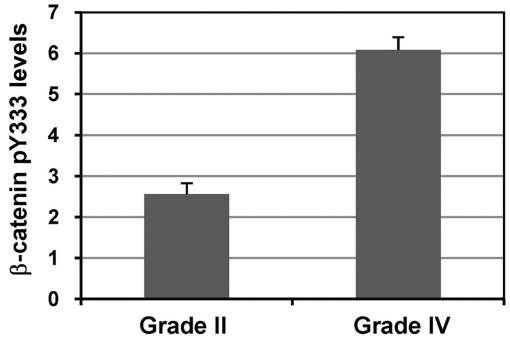

Supplementary Figure 21. The levels of c-Src Y418 phosphorylation correlate with grades of glioma malignancy.

Immunohistochemical staining of 30 diffuse astrocytoma specimens with anti–phospho-β-catenin Y333 antibody was performed and analyzed by comparing it with the staining of 88 GBM specimens (Student's *t* test, two tailed, P < 0.001).

SUPPLEMENTARY DISCUSSION

In this report, we demonstrate that PKM2, but not PKM1, in response to EGF, translocates into the nucleus and binds to c-Src-phosphorylated β-catenin at Y333, thereby directly regulating β-catenin-dependent gene expression (Supplementary Fig. 1). Pretreatment with cycloheximide, which blocks protein translation and thereby excludes the potential effect of transcriptionally regulated protein expression on subcellular redistribution of proteins, did not inhibit EGF-induced PKM2 nuclear accumulation (Supplementary Fig. 2b, right panel). These results suggest that EGF induces the nuclear translocation of PKM2 independent of changes in PKM2 expression.

To examine whether cytokines or other growth factors have a similar effect to that of EGF stimulation, we treated U87 cells with interleukin 3, fibroblast growth factor, and platelet-derived growth factor. These treatments induced STAT3 phosphorylation, but failed to induce β-catenin Y333 phosphorylation or the PKM2–β-catenin interaction (data not shown), suggesting that IL3, FGF, and PDGF do not regulate β-catenin similarly to EGF.

β-catenin can be phosphorylated at multiple tyrosine residues by distinct protein kinases[28]. Protein tyrosine kinase 6 (PTK6) primarily phosphorylates β-catenin at Y64, which exerts no effect on PTK6-inhibited β-catenin transcriptional activity[29]. Bcr-ABL phosphorylates β-catenin at Y86 and Y654 and prevents β-catenin from binding to axin/GSK-3β and subsequent phosphorylation by GSK-3β, thereby enhancing the stability of β-catenin[12]. In an in vitro experiment, purified β-catenin can be phosphorylated by recombinant c-Src, primarily at Y86, in addition to Y654. Phosphorylation of Y654, but not Y86, prevents β-catenin from binding to E-cadherin in vitro[30] or in response to UV irradiation[31]. However, c-Src-dependent β-catenin phosphorylation at these residues has not been validated in vivo. Our results show that c-Src phosphorylates β-catenin at Y333 in vitro and that β-catenin Y333F is largely resistant to c-Src-mediated phosphorylation. In addition, inhibition or deficiency of c-Src or mutation of β-catenin Y333, but not of Y86, blocked EGF-induced nuclear β-catenin phosphorylation. The Src-dependent phosphorylation of β-catenin at Y333 in the nucleus was further validated by experiments using an antibody that could specifically recognize the phosphorylated Y333 of β-catenin. In combination with the evidence that EGF treatment resulted in nuclear translocation of c-Src and an increase in binding of c-Src to nuclear β-catenin, these results indicate that nuclear β-catenin is a physiological substrate of c-Src in response to EGF stimulation. Since co-IP experiments did not detect any associated PKM2 and c-Src (data not shown), it suggests that c-

Src disassociates from β-catenin after β-catenin phosphorylation and does not complex with PKM2.

Reconstituted expression of PKM2 K433E and β-catenin Y333F failed to induce tumorigenesis. PKM2 K433E mutation may affect the status of PKM2 oligomerization in cells and the ability of the cells to modulate glycolytic flux[9,32,33]. Given that binding of phosphorylated β-catenin Y333 to PKM2 likely contributes to the release of PKM2 allosteric activator FBP and reduces PKM2 activity[9] in the nucleus, expression of β-catenin Y333F could also affect glycolysis if unbound and more active PKM2 exits the nucleus. That PKM2 modulates histone H3 acetylation, thereby downstream gene expression, may indirectly regulate cancer cell metabolism that also contributes to tumorigenesis. However, the defect of PKM2 K433E in promoting tumorigenesis was rescued by Wnt1 expression, supporting the essential role of PKM2-regulated β-catenin transactivation in EGFR-promoted tumor development. The finding of phosphorylation of β-catenin Y333 by c-Src in the nucleus with subsequent interaction with PKM2 indicates that subcellular compartment-specific modification of β-catenin defines its interacting proteins and thereby its functions. β-catenin Y333 phosphorylation is an independent predictor of glioma malignancy, and GBM patient survival distinguishes it as a potential biomarker for both prognosis and selection of GBM treatment with Src inhibitors in clinical practice.

SUPPLEMENTARY REFERENCES

27. Chou, A.H. & Howard, B.D. Inhibition by Wnt-1 or Wnt-3a of nerve growth factor-induced differentiation of PC12 cells is reversed by bisindolylmaleimide-I but not by several other PKC inhibitors. *Oncogene* **21,** 6348-6355 (2002).
28. Lilien, J. & Balsamo, J. The regulation of cadherin-mediated adhesion by tyrosine phosphorylation/dephosphorylation of beta-catenin. *Curr Opin Cell Biol* **17,** 459-465 (2005).
29. Palka-Hamblin, H.L. *et al.* Identification of beta-catenin as a target of the intracellular tyrosine kinase PTK6. *J Cell Sci* **123,** 236-245.
30. Roura, S., Miravet, S., Piedra, J., Garcia de Herreros, A. & Dunach, M. Regulation of E-cadherin/Catenin association by tyrosine phosphorylation. *J Biol Chem* **274,** 36734-36740 (1999).
31. Jean, C. *et al.* Epidermal growth factor receptor/beta-catenin/T-cell factor 4/matrix metalloproteinase 1: a new pathway for regulating keratinocyte invasiveness after UVA irradiation. *Cancer Res* **69,** 3291-3299 (2009).
32. Jurica, M.S. *et al.* The allosteric regulation of pyruvate kinase by fructose-1,6-bisphosphate. *Structure* **6,** 195-210 (1998).
33. Mellati, A.A., Yucel, M., Altinors, N. & Gunduz, U. Regulation of M2-type pyruvate kinase from human meningioma by allosteric effectors fructose 1,6 diphosphate and L-alanine. *Cancer Biochem Biophys* **13,** 33-41 (1992).